minerals

MDPI

Article

Role of the Down-Bending Plate as a Detrital Source in Convergent Systems Revealed by U–Pb Dating of Zircon Grains: Insights from the Southern Andes and Western Italian Alps

Andrea Di Giulio [1], Chiara Amadori [1,*], Pierre Mueller [1] and Antonio Langone [2]

[1] Department of Earth and Environmental Sciences, University of Pavia, 27100 Pavia, Italy; andrea.digiulio@unipv.it (A.D.G.); pierre.mueller01@universitadipavia.it (P.M.)

[2] Institute of Geosciences and Earth Resources, National Research Council (C.N.R), 27100 Pavia, Italy; langone@crystal.unipv.it

* Correspondence: chiara.amadori@unipv.it

Received: 27 April 2020; Accepted: 13 July 2020; Published: 16 July 2020

Abstract: In convergent zones, several parts of the geodynamic system (e.g., continental margins, back-arc regions) can be deformed, uplifted, and eroded through time, each of them potentially delivering clastic sediments to neighboring basins. Tectonically driven events are mostly recorded in syntectonic clastic systems accumulated into different kinds of basins: trench, fore-arc, and back-arc basins in subduction zones and foredeep, thrust-top, and episutural basins in collisional settings. The most widely used tools for provenance analysis of synorogenic sediments and for unraveling the tectonic evolution of convergent zones are sandstone petrography and U–Pb dating of detrital zircon. In this paper, we present a comparison of previously published data discussing how these techniques are used to constrain provenance reconstructions and contribute to a better understanding of the tectonic evolution of (i) the Cretaceous transition from extensional to compressional regimes in the back-arc region of the southern Andean system; and (ii) the involvement of the passive European continental margin in the Western Alps subduction system during impending Alpine collision. In both cases, sediments delivered from the down-bending continental block are significantly involved. Our findings highlight its role as a detrital source, which is generally underestimated or even ignored in current tectonic models.

Keywords: subduction zones; U–Pb dating; sandstone petrography; provenance; peripheral bulge; tectonics

1. Introduction

Detrital petrology studies of sedimentary basin fill can yield insights into the tectonics that govern compressional settings. Convergent zones are characterized by tectonically active regions affected by exhumation, uplift, and erosion and are surrounded by synorogenic basins accommodating clastic sediments produced in these zones [1,2]. This leads to complex source-to-sink systems where a relatively continuous transfer of rock mass tries to keep the system in equilibrium (i.e., growing relief vs. erosion) [3,4]. Although orogenic prisms are generally thought to be the main (if not the unique) source for detrital sediments in convergent zones, other parts of geodynamic systems can be involved when exhumated [5,6]. Such conditions are met in the cases of the foreland sector in the back-arc area of Andean-type subduction zones or in that of the passive continental margin of a down-bending continental block arriving near a subduction front during the final steps of oceanic closure. Traditionally, the tectonic evolution of those source-to-sink systems is studied by

the provenance analysis of clastic sediments accumulated in synorogenic basins, commonly used to decipher the history of eroded units from their erosional products. These studies include a variety of tools whose choice depends on a number of factors like the expected lithology of eroded rocks, the grain size of eroded sediment (gravel vs. sand vs. mud), and so forth. Among these tools, spanning from pebble clast petrology to mudstone and isotope geochemistry (i.e., Sm–Nd and Rb–Sr systems, [7]), the geo-thermochronology of specific types of sand-size clastic heavy minerals has rapidly developed and is now a standardized procedure (see [8] for an up-to-date review).

Nevertheless, we emphasize the importance of combining U–Pb dating of detrital zircons with sandstone petrography in order to (i) obtain a more complete picture of the parent rocks exposed in the source areas, including rock types lacking zircon crystals (e.g., carbonate rocks, basic and ultrabasic rocks, etc.); (ii) identify possible evidence of clastic grain recycling [9,10], which could potentially modify the interpretation of geochronological results; and (iii) analyze sediment composition and maturity, used as a tracer for source region relief and changes in climate of the source terrane (see [11] for an updated review).

Here, we present the results of two different studies in which U–Pb dating of detrital zircon grains, combined with other analytical approaches, has been employed to reconstruct the tectonic evolution of the convergent systems of the Southern Andes and the Western Italian Alps during some key and transient steps of their tectonic transformation. In particular, we describe the contribution of clastic zircon U–Pb geochronology for deciphering the signature with syntectonic sediments left by (i) the late Cretaceous transition from an extensional to a compressional retro-arc foreland basin of the Neuquén Basin in the Southern Andean region [12–15] and (ii) the Late Cretaceous final stages of subduction and related oceanic closure preceding the onset of continental collision in the Ligurian sector of the Western Italian Alps [16–18]. In both cases, results document the importance of the down-bending plate as a voluminous detrital source. Due to its low relief and the low degree of internal deformation, the provenance signal of the down-bending plate appears either underrepresented or absent to undetectable in the detrital record. However, when deduced, it may be linked to a flexural uplift response driven by the interplay between lithospheric properties of the plate (i.e., elastic thickness) [19] and the ensuing evolution of the drainage pattern [20].

2. Materials and Methods

In both presented case studies, the approach is based on provenance analyses of sandstone samples. Among the variety of tools available to address the scientific questions, we preferred to couple U–Pb radiometric age determination of detrital zircon grains with the standard point-counting analysis of sandstone framework grains.

U–Pb dating of detrital zircon grains has become a relatively standard approach for provenance study of clastic systems due to (i) the commonness of zircon crystals in parent rocks, and its resistance to diagenesis results in the relative abundance of zircon grains in clastic sedimentary rocks [21]; and (ii) its relatively low cost, allowing the collection of a statistically significant number of data (commonly >100) necessary for its application to clastic systems. In both presented case studies, U–Pb dating of detrital zircons was performed after the following standard procedure for sample preparation and heavy mineral separation. Sandstones were first crushed and then sieved between 300 and 63 microns. Zircon separates were prepared using heavy liquids and magnetic separation, then they were hand-picked under a binocular microscope, mounted into epoxy resin, and polished down to 0.25 microns to reveal the inner structures of zircon grains. This generalized sequence of steps is also suitable for apatite fission track analysis [22]. Prior to isotopic characterization, the internal structure of zircon was investigated under cathodoluminescence and the most suitable areas for the analysis were selected (see [12] for a detailed description of the morphology of the zircon grains). Rim and core ages [12,14] were collected to discriminate magmatic and metamorphic source rocks only during the deposition and evolution of the Neuquén group. For this reason, samples below the regional unconformity (i.e., Rayoso Formation at the base of the Neuquén Group) were not better investigated. U–Pb ratios in samples were determined with laser ablation inductively coupled plasma mass spectrometry (LA-MC-ICPMS) following the method described in [23] and [24].

In the Andean case, U–Pb geochronology was performed at Laboratorio de Geocronologia, Universitade de Brasilia (Brazil), following the method described in Matteini et al. [20] (Table S1), whereas U–Pb dating on detrital zircon from the Western Alps was performed at the LA-MC-ICPMS laboratory of the IGG-CNR of Pavia (Italy) following the method described in Tiepolo et al. [24] (Table S2).

When possible, 100 zircon grains of each sample were dated. As a whole, 325 (out of 512 analyzed) zircon grains for the Andean case and 356 (out of 432 zircon grain spots analyzed) for the Western Alps case were used. For the Andean case, only concordant or subconcordant (discordance smaller than ±3%) ages were considered, whereas for the Western Alps case, U–Pb ages with a discordance smaller than ±10% were considered as reliable. $^{206}Pb/^{238}U$ ages were used for grains younger than 1.2 Ga and $^{206}Pb/^{207}Pb$ for grains older than 1.2 Ga (see [12,14,17,18] and Tables S1 and S2).

Sandstone petrography was investigated through a standard thin-section point counting routine, following the Gazzi–Dickinson method [25,26] in order to minimize the possible bias introduced by different grain sizes of the studied samples [11,27]. According to the method, a double-point counting was performed on each sample, dealing with all rock constituents (framework grains, matrix, cements, pores; at least 250 framework grains counted) and fine-grained rock fragments (at least 200 fine-grained rock fragments counted) as proposed and described in detail by Cibin et al. [28] (Table S3). The goal of such double-point counting is to get a better picture of the rock types exposed in the source region and their tectonic meaning in terms of traditional provenance categories [29], including the occurrence of sedimentary rocks which could potentially deliver second-cycle zircon grains. As a whole, 33 thin sections were analyzed in the Andean case and 72 in the Western Alps case [14,17,18].

In the Southern Andes case study, thermochronological data from apatite grains were collected in order to provide a multiproxy dataset. Apatite fission track (AFT) and single-grain double-dating (AFT and U–Pb geochronology on the same grain) were performed to constrain the *T*–*t* path (temperature–time or cooling history) of rocks, both source and basin filling, with respect to a temperature range of 60–110 °C, called the Partial Annealing Zone (PAZ) [30,31]. Since fission tracks anneal primarily as a function of temperature, such that at temperatures higher than 110 ± 10 °C tracks are entirely annealed, temperatures cooler than 60 °C lead to minimal track annealing [32]. AFT analysis was performed on three samples where ~100 grains were analyzed for each detrital sample. Unfortunately, there were not enough confined lengths present in any given population to be statistically significant, so length data are not reported. For each sample, fission track grain–age distributions and populations were determined using both the Binomfit program [33] (which applies the binomial peak-fitting method [34]) and Density Plotter [35]. Calculated populations are reported by age and error (2σ). The apatite system is very sensitive to temperatures within the upper portion of the crust, less than about 4 km, and ages can either represent cooling events by exhumation of parent rocks or "geologically instantaneous" cooling following magmatism [36]. For this reason, 23 apatite AFT data Cretaceous in age (i.e., near syndepositional) were also coupled with apatite U–Pb dating. Apatite has also been employed in high-temperature thermochronology studies, which demonstrate that the U–Pb system in apatite has a closure temperature of about 450–550 °C [37,38]. LA–MC-ICPMS U–Pb dating of apatite is more challenging, as apatite typically contains lower U and Pb concentrations. In contrast to the well-documented polycyclic behavior of the stable heavy mineral zircon, apatite is unstable in acidic groundwater and weathering profiles, and it merely shows limited mechanical stability in sedimentary transport systems. Thus, it more likely represents first-cycle detritus; hence, U–Pb apatite dating would yield complementary information to U–Pb zircon provenance studies. Fission track and U–Pb dating are, therefore, two of the most useful and rapid techniques in apatite provenance studies. They yield complementary information, with the apatite fission track system indicating low-temperature exhumation ages and the U–Pb system yielding high-temperature cooling ages, which help constrain the timing of apatite crystallization [39,40]. Apatite U–Pb dating was conducted by laser ablation multicollector inductively coupled plasma

mass spectrometry (LA-MC-ICPMS) at the Arizona LaserChron Center, following the methods used for zircon by Gehrels et al. [41,42] and Gehrels [43], modified for apatite by Thomson et al. [44].

3. Geological Framework and Results of the Southern Andes and Western Italian Alps Case Studies

3.1. The Case of the Retro-Arc Basin of Southern Andes between 34° and 40° S Latitude (Neuquén Basin, Argentina)

3.1.1. Geological Setting and Stratigraphy

The Neuquén Basin is a Mesozoic–Early Cenozoic foreland basin located in a retro-arc position with respect to the Andean volcanic arc between 34° and 40° S (Figure 1A). Due to its long and fairly continuous subsidence, the basin contains an almost complete record of Mesozoic Andean tectonics, erosion, and sedimentation. The geological evolution of the Neuquén Basin was largely controlled by changes in the tectonic regime along the western margin of South America during the Mesozoic and Cenozoic eras (see [12,14,15,45–47] for an up-to-date review). In particular, the Jurassic–Cretaceous evolution has been linked to changes in the subduction slab dip of the oceanic Nazca Plate under the eastern South American continental margin, and to changes in trench roll-back velocities [46], and is characterized by (i) a Jurassic–Early Cretaceous back-arc extensional phase linked to a steeply dipping subduction and (ii) a contractional retro-arc foreland basin phase linked to a temporary shallower dipping subduction due to a change in the absolute motion of South America. The sedimentary record preserved in the continental Cretaceous strata of the Neuquén Basin allows investigating the effects of that transition from an extensional back-arc to a contractional retro-arc foreland setting, notwithstanding that no significant facies changes occurred as depositional environments remained continental with fluvial deposits during the entire Cretaceous evolution (see [14] for a detailed description of depositional facies). In particular, the investigated effects concern (i) switches in source regions of the clastic detritus; (ii) exhumation patterns of source rocks; and (iii) stratigraphic architecture of the basin. Most Cretaceous sedimentary evolution is recorded by a thick continental clastic succession formed by the Bajada del Agrio and the Neuquén Groups, separated by a regional-scale Cenomanian unconformity (Figure 1B). This continental succession has been intensively studied in order to capture the tectonic signal linked to the evolution of that portion of the Andean system.

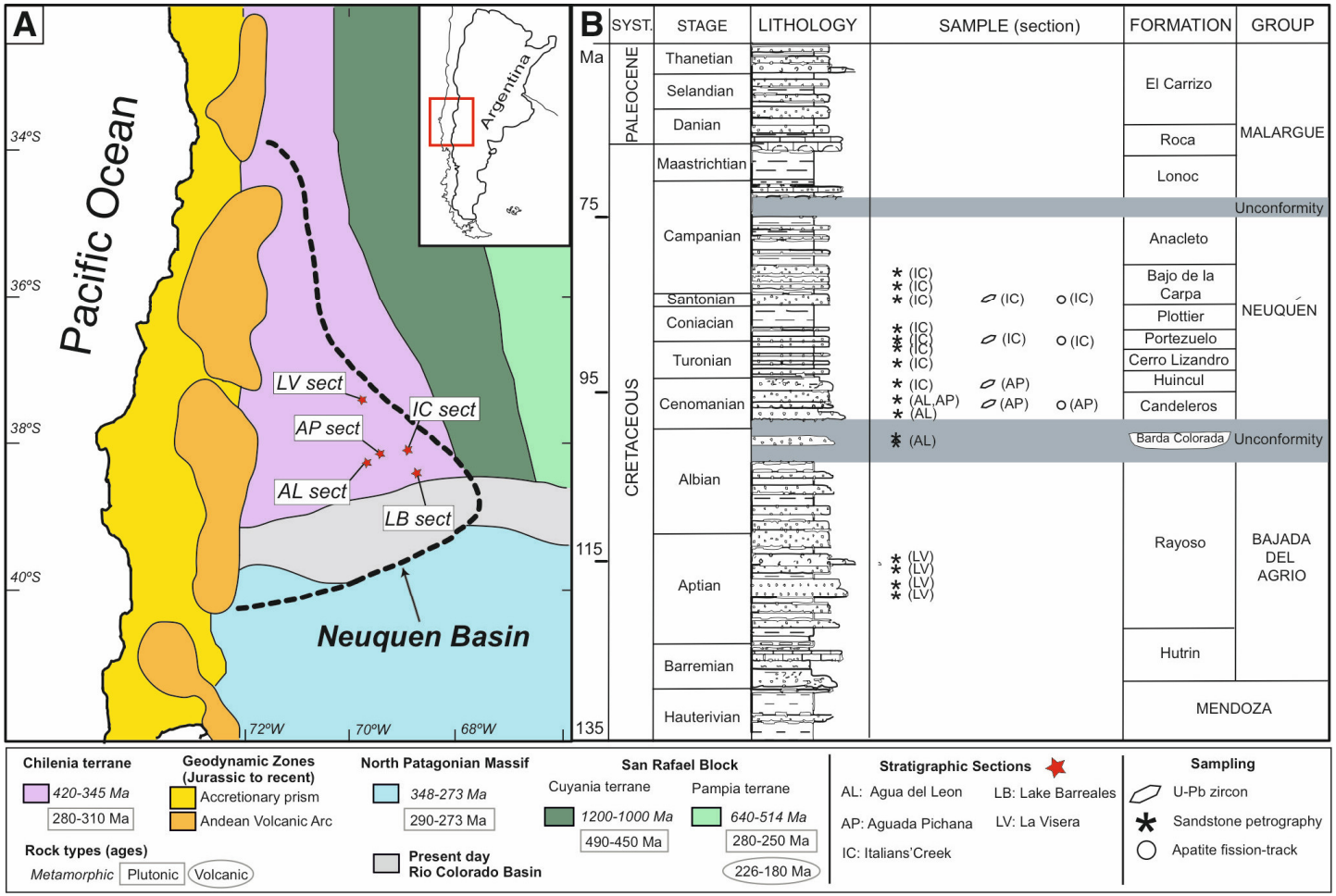

Figure 1. (**A**) Geological setting of the Neuquén Basin in the back-arc region of Southern Andes between 40° and 36° S latitude with locations of the sampled sections (modified after [48]). (**B**) Stratigraphy of the Cretaceous and lower Cenozoic filling of the Neuquén Basin with stratigraphic positions of the studied samples. Modified after [14], where also references on geochronological ages for different source terranes are reported.

3.1.2. The Detrital Record from Detrital Zircon U–Pb Dating, Sandstone Petrography, and Thermochronological Proxies

Sandstone provenance has been intensively studied in the last 10 years in the Andean retro-arc basins, frequently using U–Pb dating of zircon grains as the main or unique approach [13–16,47–51]; however, many of these geochronological studies concern the Meso-Cenozoic sedimentary sequences of the northern and southern sector of Andean mountain building [13,52–56]. Here, we particularly focus on the data reported in the regional studies by Di Giulio et al. [14,16]. These studies, performed on the Cretaceous part of the Neuquén Basin, reveal a distinct shift in sandstone provenance related to a change in source exhumation patterns of parent rocks as well as lag time across the basin-scale pre-Cenomanian unconformity that divides the Bajada del Agrio and the Neuquén Groups [13,14] (Figure 1B). Sandstone petrography of the same stratigraphic interval consistently shows a shift from a mixed to a volcanic arc signature across the Cenomanian unconformity that divides the Rajoso from the Candeleros Formation, and it shows a progressive return toward a mixed and then to cratonic signature along the Neuquén Group (Figure 2A). More specifically, sandstone detrital mode changes mostly reflect the variable abundance of fine-grained volcanic rock fragments in the studied formations, reaching a maximum in the lower Candeleros Formation and then rapidly decreasing up-section in the Neuquén Group. Consistently, U–Pb dating of zircon grains from clastic units across the unconformity in the Rayoso Formation and then along the Neuquén Group distinctly records an abrupt change of detrital age populations.

In the Neuquén Basin, from the Candeleros Formation, zircon grains age populations show a massive arrival of crystals with cooling ages equal or very close to the depositional age (few tens of millions to zero years of difference). This contribution is from syndepositional volcanics and/or juvenile volcanic material completely absent before (Rayoso Formation; Figure 2B,C). In the Rayoso Formation, the difference in time between its depositional age (Aptian–Albian) and the youngest detrital zircon population is ca. 100 Ma. Furthermore, the cumulative curve (Figure 2B) of the Rayoso Formation shows that most of the measured crystallization zircon ages are 250 Ma older than the depositional age as expected in tectonic settings characterized by erosion of old basement rocks.

Up-section (above Candeleros Formation), the progressive decrease of syndepositional volcanics and/or juvenile volcanic material is visible, as well as substitution by older zircon grains (Figure 2B,C). The picture is completed by geo-thermochronological data on apatite grains (U–Pb dating and fission tracks), that is, the double-dating method (Figure 3). Double-dating of apatite crystals was preliminarily used to detect possible synsedimentary volcanic contributions because AFT data is useful for unravelling the exhumation story of parent rocks within the upper few kilometers (i.e., their exhumation above the AFT annealing temperature). The results (Figure 3B) show that most of the analyzed apatite grains had a nonvolcanic origin, as their U–Pb and AFT ages were significantly different (delta age spanning from 150 to more than 300 Ma). Only one exception showed zero delta age between U–Pb and AFT ages, thus confirming its volcanic origin. For the nonvolcanic apatite grains, two broadly different age populations can be recognized and interpreted as two different source regions with respect to their tectonic history and lag time, defined as the difference between the AFT age and the depositional age of the rock. The sources are: (1) a rapidly exhuming region delivering apatite grains with AFT ages very close to the depositional age (very short lag time, ca. 10–20 Ma), shown by the single peak in Candeleros Formation (123.7 ± 4.7 Ma) and the youngest peak in Portezuelo and Bajo de la Carpa Formations (82.4 ± 5.5 and 94.7 ± 4.7 Ma, respectively), and (2) a sector delivering apatite grains with AFT ages several tens of Ma (>50 Ma) older than the depositional age of samples. This is inferred by the presence of a second older population in Portezuelo and Bajo de la Carpa Formations (158.3 ± 7.7 and 163 ± 9.5 Ma, respectively). Generally, a longer lag time testifies to the erosion of rocks that remained above the AFT annealing temperature for a considerably long time before arriving at the surface [36]; in addition, the proportion of the second source increases up-section (Figure 3A).

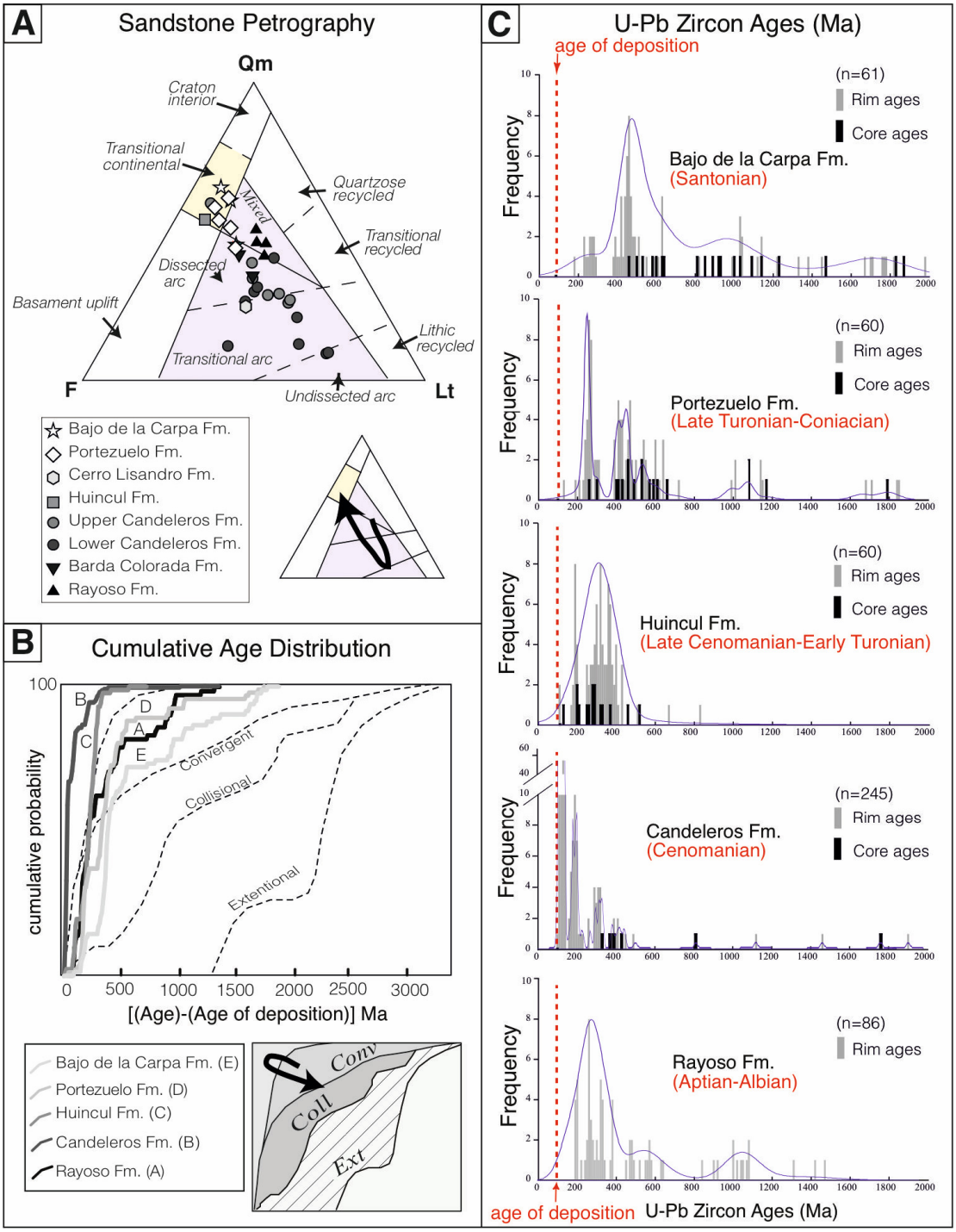

Figure 2. (**A**) Sandstone petrography in the Cretaceous Bajada del Agrio and Neuquén Groups of Neuquén Basin plotted in the QmFLt provenance diagram of Dickinson [29]. (**B**) Results from U–Pb dating of detrital zircons. Cumulative proportion curves showing the difference between the crystallization age for a detrital zircon and the depositional age of the sample in which it occurs. Solid lines indicate the studied samples; dashed lines bind the fields representing three tectonic settings as defined in [50]. (**C**) U–Pb ages (bins 10 Ma) shown from top to bottom according to their stratigraphic order (Table S1). Blue line is the kernel density estimate (KDE). Red text is the depositional age of the corresponding formations (see [14] and reference therein for the paleontological and geochronological data). For the stratigraphic position of studied samples, refer to Figure 1B. Modified from [14]. Stratigraphic positions of samples are reported in Figure 1B.

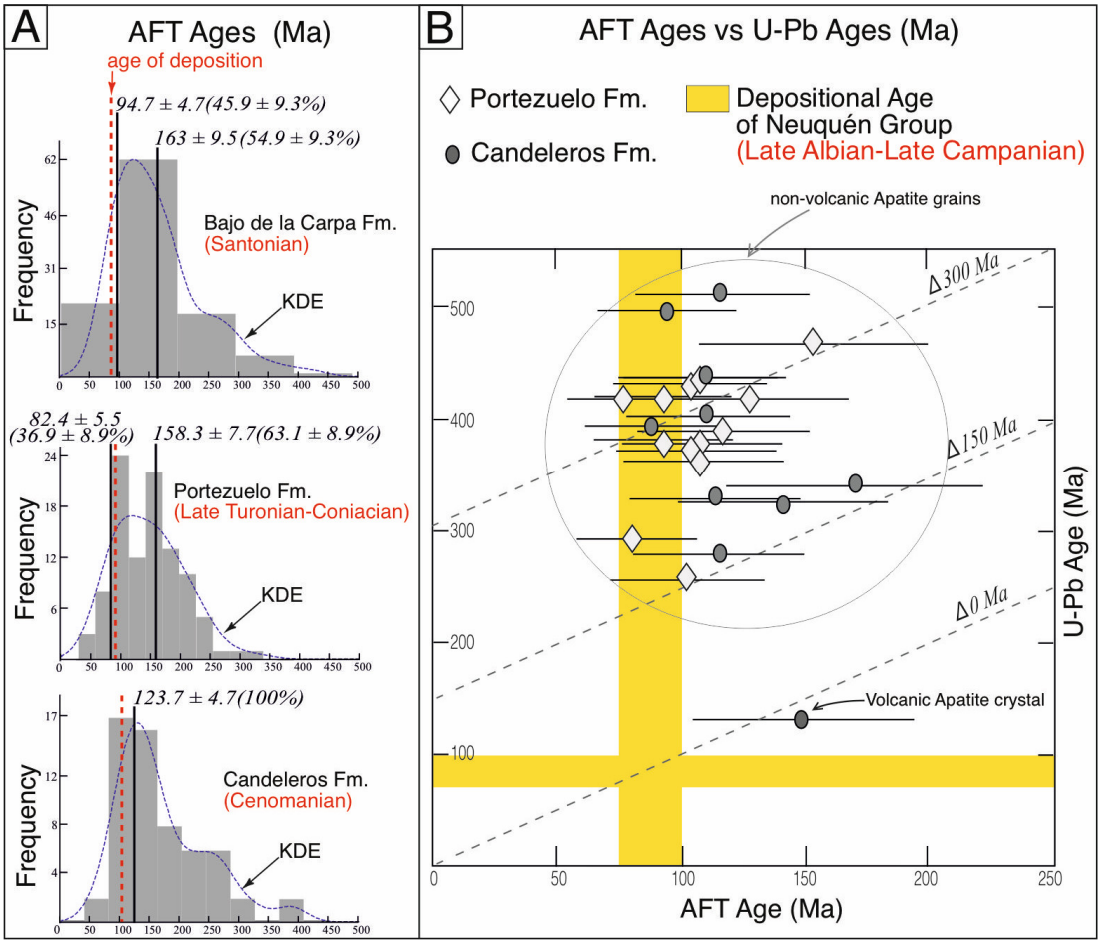

Figure 3. (**A**) Kernel density estimate (KDE, dashed blue line) and histogram distributions (grey rectangles) from apatite fission track data produced using Density Plotter [35] from Bajo de la Carpa, Portezuelo, and Candeleros Formations, shown in their stratigraphic order. Calculated populations are reported by age and error 2σ. (**B**) Results of double-dating on detrital apatite grains from the Neuquén Group; sample stratigraphic positions reported in Figure 1B. Note that no volcanic crystals (delta age = 0) are recognizable, with only one exception in the Candeleros Formation. Red text is the age of deposition (see [14] and reference therein for the paleontological and geochronological data).

3.1.3. Discussion on the Drainage Evolution and Related Provenance Changes in the Neuquén Basin

The collected multiproxy dataset allows tracing the tectonic evolution and the related rearrangement of the drainage pattern within the source-to-sink routing system formed by the Neuquén retro-arc basin and the Andean cordillera, between 36° and 40° S latitude from Albian to Santonian time. This evolution can be schematically summarized in the following main steps. During Albian time, the existence of a divergent drainage pattern in a back-arc basin setting is suggested by the lack of syndepositional, neovolcanic grains (Aptian–Albian in age) in the Rayoso Formation, as recorded by coupled zircon U–Pb ages, cumulative curve, and sandstone petrography (Figure 2).

In fact, at that time (>100 Ma), a volcanic arc was active and its overall detritus was likely transported westward, towards the pacific margin, with the only exception of ash layers. A volcanic detritus transported eastward would have needed to pass over the rift shoulders to finally end up in the basin; in this case, it would have been recorded by detrital zircon ages coeval with the sediments' depositional age. By contrast, the back-arc Neuquén Basin was mostly fed by the uplifted rift shoulders, mainly composed of Paleozoic–Proterozoic basement rocks and their Jurassic–Triassic covers shown by the highest peak of U–Pb zircon ages in the Rayoso Formation between ca. 200 and 400 Ma and minor peaks around 500–600 Ma and ca. 1.1 Ga (Figure 2C). At around 100 Ma, the region

started to become affected by contractional deformation, possibly linked to the global-scale plate reorganization produced by the opening of the Southern Atlantic Ocean [57] (see also [15] for discussion). In the Neuquén Basin, this tectonic inversion triggered a rapid reorganization of the drainage pattern caused by the transition from a back-arc extensional setting to a retro-arc contractional basin. In the stratigraphic record, this transition is marked by the pre-Cenomanian regional-scale erosional unconformity between the Bajada del Agrio Group and the Neuquén Group occurring in an otherwise continuously subsiding basin. This erosion is thought to be the result of a weak but basin-scale uplift, due to large-scale continental folding (i.e., buckling) during the very beginning of contraction, before the full development of thrust tectonics and an adjacent foreland basin. After this uplift event, during Cenomanian–Turonian time (Candeleros, Huincul, and Portezuelo Formations), continental deposition restarted and both zircon U–Pb ages (highest peak at ca. 95–150 Ma in the Candeleros Formation) and sandstone petrography (volcanic lithic-rich) consistently recorded an important and abrupt shift, with poorly dissected syndepositional volcanic arc detritus (Figure 2A) arriving in the Neuquén Basin from the Cordillera together with a minor but ongoing contribution from Mesozoic (ca. 200 Ma detrital zircon age peak) and Paleozoic rocks exhumed during the Cretaceous (zircon ages of ca. 300–500 Ma) (Figure 2C). Paleocurrent data in the Neuquén Group show N–S to E–NE directions moving up-section [14] and allows confirming this reconstruction.

This evidence is interpreted as recording the beginning of contractional-related exhumation of the Cordillera, coupled with inversion of the drainage pattern from divergent to convergent and linked to transition of the Neuquén Basin from a back-arc to a retro-arc foreland basin. After this step, during the Late Cretaceous evolution, the integration of U–Pb zircon dating, sandstone petrography, and apatite double-dating results (showing no volcanic apatite grains deposited in the Neuquén group, except for only one crystal in the lower Candeleros Formation, Figure 3B) suggests a progressive increase of detrital input from old basement rocks. This included Proterozoic rocks with a multistage magmatic–metamorphic history (>500 Ma, rim-core ages, Figure 2C) exhumed during the Jurassic, together with a contribution from rocks that suffered Cretaceous exhumation with removal of the partial annealing zone during the Cenomanian (i.e., older AFT populations, Figure 3A), followed by increasing tectonic exhumation up to Santonian time. As proposed by [12] and [14], this multiproxy dataset indicates that a convergent drainage pattern developed into a contractional foreland setting during deposition of the Neuquén Group, with detrital material supplied by both the Andean Cordillera to the west and by the craton to the east, which was uplifted during eastward migration of the flexural peripheral bulge causing an increasing detrital contribution from the San Rafael continental block located in the foreland.

3.2. The Case of the Western Ligurian Flysch (NW Italy) during Impending Collision

3.2.1. Geological Setting and Stratigraphy

This case study addresses the detrital provenance of the terrigenous units included in the Cretaceous–Paleocene Western Ligurian Helminthoid Flysch Complex (WLF), which forms the uppermost part of the nappe pile of the Ligurian part of the Western Italian Alps, NW Italy (Figure 4A). The WLF represents the remnant of the accretionary wedge formed by the cover of the Piedmont–Ligurian ocean and its continental margin, scraped off along the Ligurian Alps transect of the Alpine subduction system in the framework of an intra-oceanic subduction zone [16,58–60] (Figure 4B–D). During the Late Eocene–Early Oligocene continental collision, the WLF was thrust over the European foreland and presently rests on the Mesozoic Dauphinois–Provençal succession to the west and southwest and on the Briançonnais units of the Ligurian Alps to the north [16,59,61–63]. The WFL comprises four main flysch units (from top to bottom of the complex): the San Remo–Monte Saccarello Unit, the Moglio–Testico Unit, the Borghetto d'Arroscia Unit, and the Colla Domenica–Leverone Unit (Figure 4B,C). The tectonically inverted chronostratigraphic organization of these units, divided by southward dipping thrusts, with the oldest unit resting on top of the nappe pile, documents the typical tectonic inversion of accretionary wedges [16,64]. Whilst the three lowermost

and younger units underwent multiphase, ductile–brittle deformation, the oldest and structurally topmost San Remo–Monte Saccarello Unit is characterized by a rather simple and less intense structural overprint.

Two of the units of the WFL feature poorly dated upper Cretaceous, thick, sandstone-rich turbidite units [16] (Figure 4B): (i) The Borghetto d'Arroscia Unit contains quartz-rich turbidite fan deposits of the Monte Bignone Formation (sometimes called M. Bignone Quartzites in the regional literature) [65] interbedded with conglomeratic levels primarily comprising carbonate clasts [66], and divided by one of these conglomerate units into a lower and an upper quartzite member. (ii) The San Remo–Monte Saccarello Unit contains quartz-rich sandy turbidites in the uppermost part of the lowermost stratigraphic unit (San Bartolomeo Formation) that is stratigraphically overlain by a thick sand-rich turbidite fan unit, the Bordighera Sandstone [67]. The other WFL units are composed of shaly formations at the base (sometimes called basal complexes in the regional literature: Colla Domenica Shale, Ranzo Shale, Moglio Shale, lowermost part of the S. Bartolomeo Formation) and thick and monotonous calcareous-marly flysch successions (Leverone Formation, Ubaga Limestone, Testico Formation, San Remo Flysch) of the wide family of the Alpine Helminthoid Flysches.

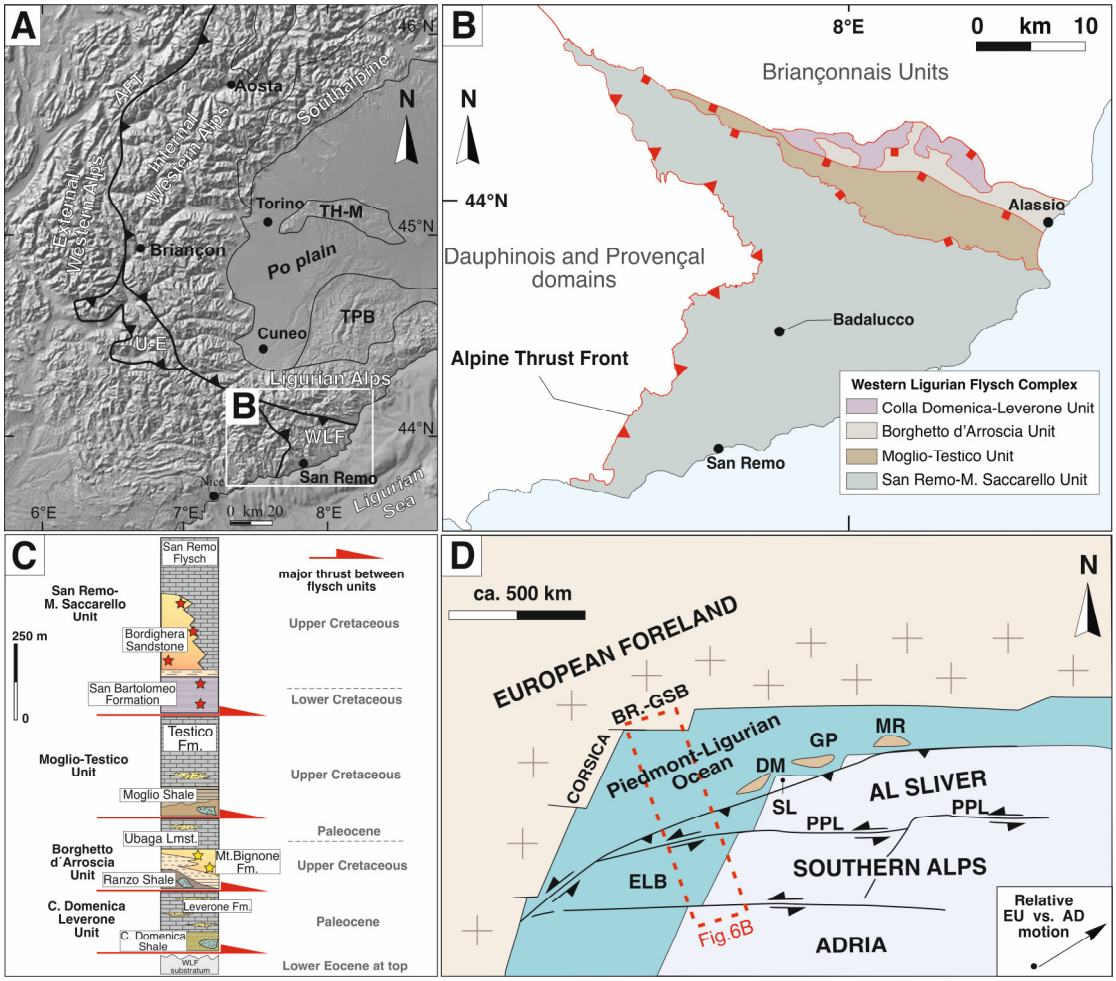

Figure 4. (**A**) Tectonic scheme of the Western Alps and location of Western Ligurian Flysch Complex (WLF); ATF: Alpine Thrust Front; U-E: Ubaye–Embrunais nappe; TH-M: Torino Hills–Monferrato arc; TPB: Tertiary Piedmont Basin. (**B**) Structural scheme of the WLF. (**C**) Stratigraphic framework of the WLF units and stratigraphic position of studied samples. (**D**) Paleogeographic reconstruction proposed for the Late Cretaceous setting of the Piedmont–Ligurian subduction zone along the Ligurian Alps transect, redrawn after [48]; BR-GSB: Briançonnais–Gran San Bernard domain; DM-GP-MR: Dora Maira–Gran Paradiso–Monte Rosa blocks; SL: Sesia–Lanzo zone; PPL: Paleo-Periadriatic Line; ELB: External Ligurian Basin; AL: Austro-Alpine continental sliver.

3.2.2. The Detrital Record from Sandstone Petrography and U–Pb Dating of Detrital Zircon Grains

Provenance analyses of sandy siliciclastic turbiditic successions of both the San Remo–Monte Saccarello Unit and the Borghetto d´Arroscia Unit were performed by means of integrating U–Pb detrital zircon chronology and sandstone petrography (Tables S2 and S4). For petrographic investigations, a total of 40 samples were acquired from the terrigenous units of the San Remo–Monte Saccarello Unit. Thirty sandstone samples were selected from two stratigraphic intervals of the Monte Bignone Formation in the Borghetto d´Arroscia unit: 27 samples from the Lower Quartzite member and 3 samples from the Upper Quartzites member. For detailed stratigraphic positions of samples processed for petrographic studies, the reader is referred to [14,15]. Samples for detrital zircon geochronology were collected from the same stratigraphic intervals (Figure 4C).

Based on sandstone modal analyses, the fine-grained turbidite sandstones of the San Bartolomeo Formation at the base of the San Remo Unit classify as quartz-rich sandstones (modal averages of $Qt_{69}F_{29}L_2$; Figure 5A). This relatively high compositional maturity [66] is accompanied by the well-sorted nature of the sandstone framework grains. Moderate to high roundness indicates high textural maturity. By contrast, the overlying coarse-grained Bordighera Sandstone turbidites represent typical arkoses, with roughly equal shares in quartz and feldspars (average modal composition: $Qt_{49}F_{48}L_3$), and typified by a poor sorting and angular to subangular framework grains. The high quartz proportions that typify the San Bartolomeo Formation samples suggest intense weathering of less stable feldspar grains during prolonged exposure on continental land masses and/or extended sedimentary recycling along lower-gradient areas [68]. In combination with the high textural maturity, according to traditional provenance categories [69], these observations indicate a stable craton to transitional continental provenance terrane. Further, this may include extensive shelfal areas where detrital material may have been subjected to additional textural maturation. Conversely, the abundance of unstable feldspar grains rules out such a provenance scenario for the younger coarse-grained Bordighera Sandstone [69]. Together with the markedly reduced textural composition, a first-cycle origin dominantly derived from an uplifting granitic basement block, with very minor contributions of low-grade metamorphic rocks and sedimentary rocks, may be inferred. Within both units, the dominance of monocrystalline over polycrystalline quartz is interpreted to indicate contributions of basement rocks [70,71].

Sandstones within the Borghetto d'Arroscia Unit exhibit variable degrees of sorting. Framework grains are typically subangular to rounded. The detritus generally contains high proportions of quartz, very low to low proportions of feldspar, and variable shares of rock fragments (mean $Qt_{83}F_5L_{12}$). Within this overall picture, the key observation is that modal percentages show significant variations, evolving from quartzose sandstones towards lithic and then to a lithic, subarkosic composition up-section (Figure 5A). The Lower Quartzite member sands feature high quartz proportions (average 86%), whereas quartz shares significantly decrease up-section towards the Upper Quartzite member (average 63%). On the contrary, feldspars account for relatively constant, low portions throughout the Lower Quartzite member (average 4%) but become more abundant in the Upper Quartzite unit (average 14%). A similar pattern can be observed in the shares of lithic fragments, which show an overall up-section increase (from 10% to 22% on average). In summary, a somewhat gradual change from quartz arenites to lithic arenites is recorded in the Lower Quartzite unit, delineated by an increase in the number of sedimentary and volcanic lithic fragments. By contrast, the Upper Quartzite member exhibits a further shift towards lithic subarkosic composition coupled with an increase in plutonic and metamorphic rock fragments. The high degree of compositional maturity characterizing the quartz-rich arenites of the Lower Quartzites in the Borghetto Unit implies intense sedimentary recycling [69], suggestive of temporary sediment storage along the source-to-sink pathway, similar to the interpretation of the provenance scenario obtained for the San Bartolomeo Formation in the San Remo-M. Saccarello unit. The compositional maturity could, hence, be explained by prolonged reworking in shallow marine environments along a passive margin shelf. The up-section increase of sedimentary lithic fragments in the M. Bignone Lower Quartzite member suggests progressive tectonic uplift and local denudation of a provenance terrane that, to a great extent, comprised a well-developed sedimentary cover sequence. Conversely, the

increased feldspar and plutonic fragment portions in the M. Bignone Upper Quartzite member would indicate a further shift towards an increasing basement source [69].

The observed stratigraphic trends in sandstone modal composition in both the San Remo and Borghetto Units raise the question of whether they reflect changes in sediment provenance area (i.e., a provenance shift) or imply a change in tectonic regime affecting the same source area. U–Pb dating of detrital zircon grains was performed to solve this basic provenance question and further constrain source area reconstructions. A total of 356 zircon grains from six samples coming from the San Bartolomeo Formation (two samples), Bordighera Sandstone (three samples), and Mt. Bignone Formation (one sample) yielded concordant ages. Comparisons of the investigated detrital zircon signatures revealed marked similarities (Figure 5B,C; standard statistical evaluations of similarity between samples' detrital age distributions via KS-tests and MDS diagrams are provided in [17,18]). All detrital zircon age spectra were characterized by their primary Carboniferous age contributions around ca. 300–360 Ma. Significant populations of Ordovician ages around 450 Ma and 480 Ma were also common in all samples. Additional similarities were expressed in the shared broad age population ranging from ca. 535 to 660 Ma. Noteworthy, minor Upper Pennsylvanian-Guadalupian age peaks between ca. 270 Ma and 305 Ma were exclusive to samples of the San Bartolomeo Formation.

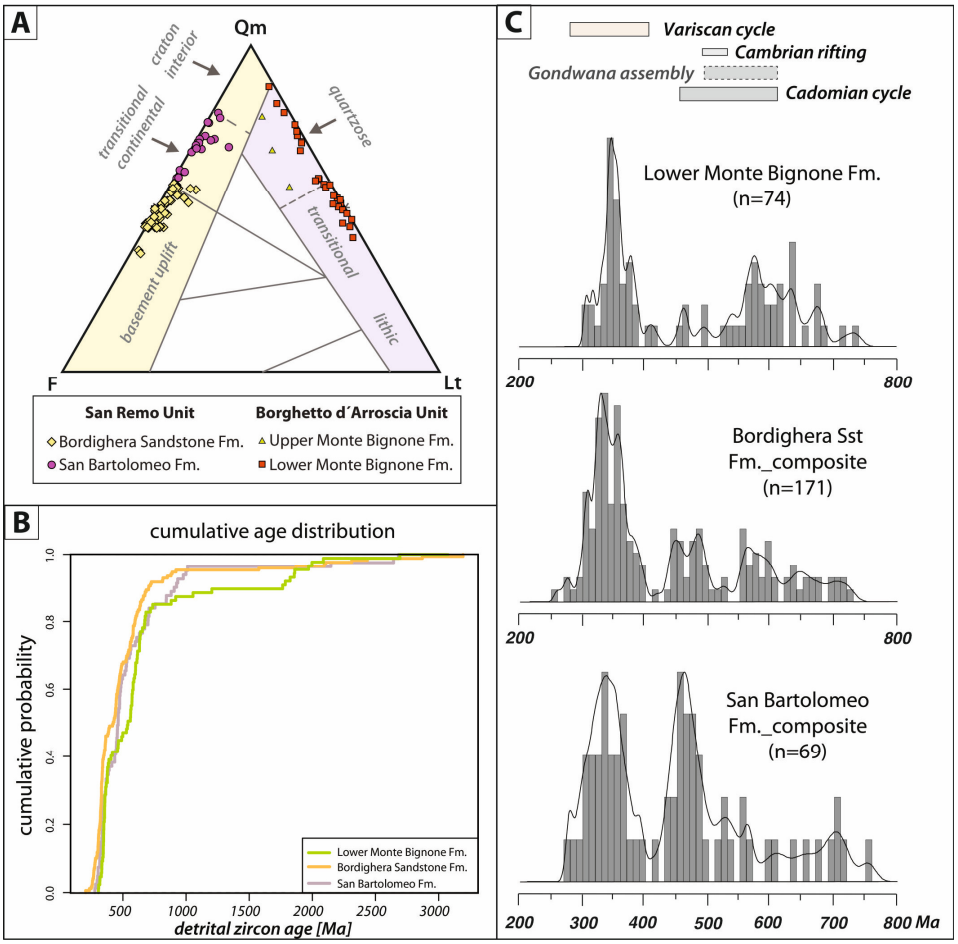

Figure 5. (**A**) Results from sandstone detrital framework analysis of the siliciclastic members of the WLF units plotted in the QmFLt provenance discrimination diagram of Dickinson [26] (Table S4:). (**B**) Compilation of cumulative detrital zircon U–Pb age distributions of the investigated siliciclastic units of the WLF. (Table S2). (**C**) Probability density plots of the siliciclastic successions of the WLF covering the time range from 200 to 800 Ma; bins 10 Ma and discordance ±10%. Note that in this case, the depositional age (Late Cretaceous) is out of the plot area, as no zircon grains with a similar age occurred in studied samples.

3.2.3. Discussion on the Erosion of the Passive Continental Margin during Oceanic Closure

The multiproxy sediment provenance study of the sandy units of the Western Ligurian Flysch Complex provides a better understanding of the precollisional evolution of the Piedmont–Ligurian ocean, and it specifically allows deciphering the role of the opposing continental margins as potential detrital sources during the final stages of oceanic closure. To this end, the distinction between the detritus delivered by the Adriatic margin (placed on the overriding plate) and that derived from the European passive margin (placed on the down-bending plate) is required.

The main populations of Carbonifeous detrital zircon U–Pb ages correspond to magmatic and metamorphic events that, in the Alpine region, occurred in the framework of the older Variscan orogeny [72]. The second most abundant age group that covers the time span between ca. 535 Ma and 660 Ma corresponds to geodynamic events associated with metamorphic and magmatic rocks that occurred in the course of the Cadomian orogeny [73]. Detrital ages between ca. 270 Ma and 305 Ma can be linked to post-Variscan magmatism associated with gravitational collapse of the thickened Variscan crust. With regard to the opposing continental margins that bounded the Piedmont Ligurian Ocean (i.e., the subducting paleo-Europe plate and the overriding Adriatic plate), pronounced late Variscan age distributions (270–330 Ma) provide fundamental insights into the provenance terrane, since granite emplacement primarily occurred along the paleo-European plate during that time span [72,74–76]; this conclusion is also supported by Multidimensional Scaling Analysis [18]. In fact, only older Variscan ages were found in Austroalpine and Carpathian basement units [77] (i.e., Adriatic plate).

These late Variscan age populations (Figure 5C) shared in all investigated clastic formations a similar provenance for all investigated WLF units. These results coupled with the detailed sedimentological description [17,18,63,67] of the clastic sequence allow inferring the principal sediment supply into the subduction zone staged from the Paleo-European continental margin (placed on the subducted plate), during its arrival close to the subduction zone facing the impending continental collision. Therefore, geochronological data provided by U–Pb detrital zircon ages helped to testify that (i) despite the observed compositional changes in sandstone modal composition, the terrigenous material was delivered by the same source terrane, and (ii) in the context of the Alpine subduction and age constraints on crustal growth stages recorded in the pre-Alpine basements [72,78], that terrane was likely placed on the passive continental margin of the subducting European plate. Nevertheless, in both investigated units, a substantial shift in tectonic stability of the source terrane was recorded first by the onset of coarse-clastic sedimentation, and then by its compositional evolution.

The development of a flexural bulge in response to the tectonic loading of the advancing Alpine accretionary wedge provides a feasible explanation for this reactivation and tectonic inversion of the lower plate margin. This would explain both the observed up-section trend in composition and the evolution of textural sediment maturity, which are interpreted to mirror the imminent arrival of the flexural bulge in the distal parts of the continental margin, triggering the reworking of quartz-rich shelf sands into the deep basin. More specifically, the up-section trend towards less mature, arkosic sands is thought to reflect the subsequent craton-ward migration (hinterland) of the flexural bulge, causing rapid unroofing of crystalline rocks and enhanced erosion rates. Increased sediment yield and sediment caliber might indicate the development of areas of high relief and/or reactivation of ancient fault scarps. The main implication from these observations is that the observed mineralogic up-section trend of decreasing sediment maturity of sediments delivered from the same source terrane can serve as a detrital tool for the inversion of the passive margin during its arrival near the subduction zone, and the forthcoming geodynamic transition from a subduction to a collisional scenario.

4. Overall Conclusions

Provenance of clastic sediments accommodated in syntectonic basins is commonly used as a tracer for reconstructing the evolution of convergent geodynamic settings. In these settings, the

orogenic prism is commonly considered as the prevailing source for detrital material. By contrast, the examples from the Andean region and Western Ligurian Alps show the following:

- In the back-arc Andean region, a transition from an extensional to a contractional setting is recorded during late Albian–early Cenomanian time (Figure 6A) by detrital provenance, possibly linked to an overall plate reorganization that caused the decrease of subduction dip. The resulting flexure of the down-bending continental block in the back-arc Andean region triggered the erosion of the South American foreland craton, providing most of the detrital material to the majority of Upper Cretaceous continental successions accommodated in the back-arc Neuquén Basin during its contractional evolution.
- In such a back-arc contractional setting, the scarceness of syndepositional volcanic zircon crystals, combined with the contrasting exhumation rate of the source rocks revealed by double apatite dating, provide clues for discriminating sediments coming from the Cordillera volcanic arc/orogenic belt from sediments staged from the continental foreland.
- In the Ligurian transect of the Western Alps (Figure 6B), an intra-oceanic subduction was supposed due to the overall lack of terrigenous material arriving in the basin during most of the Cretaceous. In such a context, the Late Cretaceous arrival of voluminous sand-size terrigenous detritus remains enigmatic.
- Coupled U–Pb dating of clastic zircon grains and sandstone petrography support the European continental margin placed on the subducting plate as the source of that material, and its arrival close to the subduction zone is thought to announce the impending collision. Within this transient phase, decreasing sandstone maturity through time is thought to record the arrival of the flexural bulge on the passive continental margin, starting from a shelf region and then moving toward the hinterland. This passage first triggered the reworking of mature quartz-rich shelf sands, and afterwards it caused basement erosion and deposition in the subduction zone of basement-sourced arkoses.

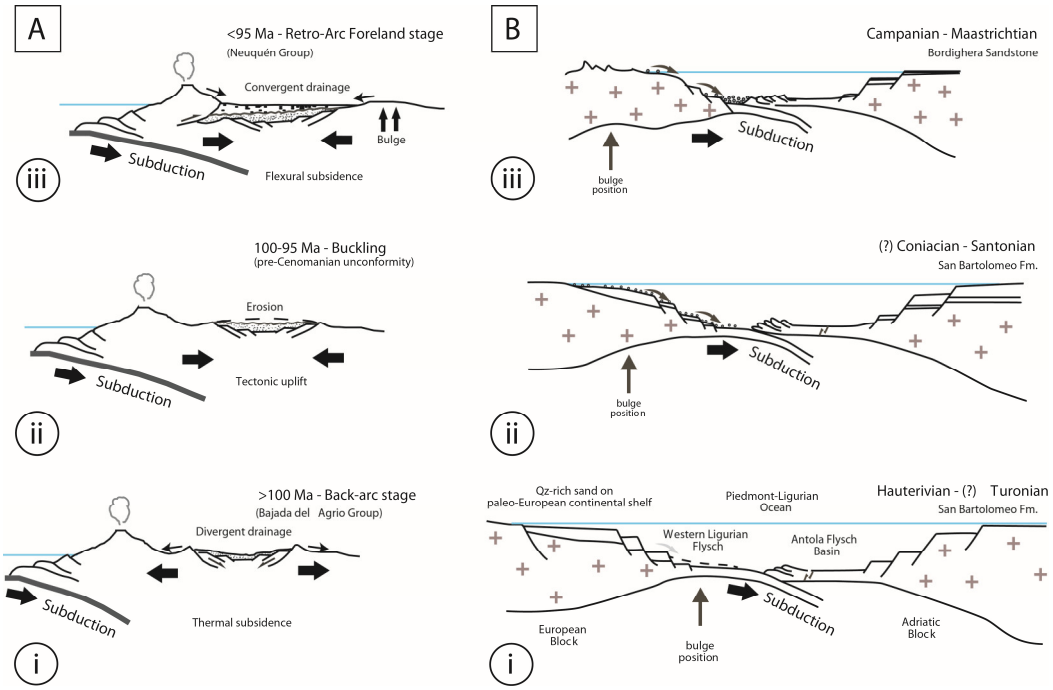

Figure 6. Tectonic model developed for the late Cretaceous evolution of (**A**) the Neuquén Basin in the retro-arc of Southern Andes, and (**B**) the Piedmont–Ligurian subduction zone along the Ligurian transect of Western Italian Alps. Note, in both, the major role of detrital source played by the continental down-bending block, uplifted and eroded by the passage of the peripheral bulge.

In summary, the findings derived from detrital studies of the south Andean system and the Ligurian transect of the Italian Alps system point out that even the down-bending block can be an important source, and sometimes even the only source, of terrigenous sediments in certain steps of the tectonic evolution of convergent systems. In the case of intra-oceanic subductions, that contribution can be considered a way to trace the final stages of oceanic closure and impending collision.

Supplementary Materials: The following are available online at www.mdpi.com/2075-163X/10/7/632/s1, Table S1: Geo-thermochronology Neuquén, Table S2: Geochronology Ligurian Alps, Table S3: Petrography Neuquén, Table S4: Petrography Ligurian Alps.

Author Contributions: A.D.G. and C.A. conceived the scientific question; P.M. and A.L. performed U–Pb zircon dating; A.D.G. and P.M. performed sandstone petrographic analyses; A.D.G., C.A., and P.M. provided figures/manuscript preparation. All authors contributed to the design of the manuscript and its final revision. All authors have read and agreed to the published version of the manuscript.

Funding: This research received no external funding.

Acknowledgments: Wilfried Winkler and Albrecht von Quadt are kindly acknowledged for inviting us to contribute to this Special Issue. All authors are indebted to two anonymous reviewers and Pereira, M.F. for their detailed and constructive revisions that led to significant improvements in the quality of the paper. We also want to thank the many colleagues that contributed to our Andean and Ligurian Alps research through the years; among them, Marco Patacci (Leeds, UK) and Victor Ramos (Buenos Aires, Argentina) are particularly acknowledged.

Conflicts of Interest: The authors declare no conflict of interest.

References

1. DeCelles, P.G.; Giles, K.A. Foreland basin systems. *Basin Res.* **1996**, *8*, 105–123, doi:10.1046/j.1365–2117.1996.01491.x.
2. Garzanti, E. The Himalayan Foreland Basin from collision onset to the present: A sedimentary–petrology perspective. *Geol. Soc. Lond. Spec. Publ.* **2019**, *483*, doi:10.1144/SP483.17.
3. Dahlen, F.A. Critical taper model of fold-and-thrust belts and accretionary wedges. *Ann. Rev. Earth Planet. Sci*. **1990**, *18*, 55–90.
4. Malevieille, J. Impact of erosion, sedimentation, and structural heritage on the structure and kinematics of orogenic wedges: Analog model and case studies. *GSA Today* **2010**, *20*, doi:10.1130/GSATG48A.1.
5. Pereira, M.F.; Chichorro, M.; Johnston, S.T.; Gutiérrez-Alonso, G.; Silva, J.B.; Linnemann, U.; Hofmann, M.; Drost, K. The missing Rheic Ocean magmatic arcs: Provenance analysis of Late Paleozoic sedimentary clastic rocks of SW Iberia. *Gondwana Res.* **2012**, *22*, 882–891.
6. Pereira, M.F.; Gutíerrez-Alonso, G.; Murphy, J.B.; Drost, K.; Gama, C.; Silva, J.B. Birth and demise of the Rheic Ocean magmatic arc(s): Combined U-Pb and Hf isotope analyses in detrital zircon from SW Iberia siliciclastic strata. *Lithos* **2017**, *278–281*, 383–399, doi:10.1016/j.lithos.2017.02.009.
7. Pereira, M.F.; Gama, C.; Dias da Silva, Í.; Fuenlabrada, J.M.; Silva, J.B.; Medina, J. Isotope geochemistry evidence for Laurussian-type sources of South-Portuguese Zone Carboniferous turbidites (Variscan orogeny). In *Pannotia to Pangea: Neoproterozoic and Paleozoic Orogenic Cycles in the Circum-North Atlantic Region*; Murphy, J.B., Ed.; Geological Society of London, Special Publication: London, UK, 2020; doi:10.1144/SP503-2019–163.
8. Malusà, M.; Fitzgerald, P.G. The geologic interpretation of the detrital thermochronology record within a stratigraphic framework, with examples from the European Alps, Taiwan and the Himalayas. *Earth Sci. Rev.* **2020**, *201*, doi:10.1016/j.earscirev.2019.103074.
9. Zuffa, G.G. Optical analyses of arenites: Influence of methodology on compositional results. In *Provenance of Arenites*; Series C; NATO Advanced Studies Institutes, Mathematical and Physical Sciences: Dordrecht, The Netherlands; Boston, MA, USA, **1985**, 165–189.
10. Di Giulio, A.; Ceriani, A.; Ghia, E.; Zucca, F. Composition of modern stream sands derived from sedimentary source rocks in a temperate climate (northern Apennines, Italy). *Sediment. Geol.* **2003**, *158*, 145–161.

11. Garzanti, E. The Maturity Myth In Sedimentology and Provenance Analysis. *J. Sediment. Res.* **2017**, *87*, 353–365, doi:10.2110/jsr.2017.17.
12. Di Giulio, A.; Ronchi, A.; Sanfilippo, A.; Tiepolo, M.; Pimentel, M.; Ramos, V.A. Detrital zircon provenance from the Neuquén Basin (south-central Andes): Cretaceous geodynamic evolution and sedimentary response in a retroarc-foreland basin. *Geology* **2012**, *40*, 559–562, doi.org/10.1130/G33052.1.
13. Horton, B.K. Sedimentary record of Andean mountain building. *Earth Sci. Rev.* **2018**, *178*, 270–309, doi:10.1016/j.earscirev.2017.11.025.
14. Di Giulio, A.; Ronchi, A.; Sanfilippo, A.; Balgord, E.A.; Carrapa, B.; Ramos, V.A. Cretaceous evolution of the Andean margin between 36 °S and 40 °S latitude through a multiproxy provenence analysis of Neuquen Basin strata (Argentina). *Basin Res.* **2017**, *29*, 284–304.doi:10.1111/bre.12176.
15. Fennell, L.M.; Iannelli, S.B.; Encinas, A.; Naipauer, M.; Valencia, V.; Folguera, A. Alternating contraction and extension in the Southern Central Andes (35 ° S–37 °S). *Am. J. Sci.* **2020**, *319*, 381–429, doi:10.2475/05.2019.02.
16. Di Giulio, A. The evolution of Western Ligurian Flysch Units and the role of mud diapirism in ancient accretionary prisms (Maritime Alps, Northwestern Italy). *Geol. Rundsch.* **1992**, *81*, 655–668.
17. Mueller, P.; Langone, A.; Patacci, M.; Di Giulio, A. Detrital signatures of impending collision: The deep-water record of the Upper Cretaceous Bordighera Sandstone and its basal complex (Ligurian Alps, Italy). *Sediment. Geol.* **2018**, *377*, 147–161, doi:10.1016/j.sedgeo.2018.10.002.
18. Mueller, P.; Langone, A.; Patacci, M.; Di Giulio, A. Towards a Southern European Tethyan Palaeomargin provenance signature: Sandstone detrital modes and detrital zircon U–Pb age distribution of the Upper Cretaceous-Paleocene Monte Bignone Sandstones (Ligurian Alps, NW Italy). *Int. J. Earth Sci.* **2019**, *109*, 201–220.
19. Burov, E.B.; Diament, M. The effective elastic thickness (te) of the continental lithosphere: What does it really mean? *J. Geophys. Res*. **1995**, *100*, 3905–3927.
20. Garcia-Castellanos, D. Interplay between lithospheric flexure and river transport in foreland basins. *Basin Res.* **2002**, *14*, 89–104.
21. Hay, D.C.; Dempster, T.J. Zircon alteration, formatin and preservation in sandstones. *Sedimentology* **2009**, *56*, 2175–2191.
22. Kohn, B.; Chung, L.; Gleadow, A. Fission-Track Analysis: Field Collection, Sample Preparation and Data Acquisition. In *Fission-Track Thermochronology and its Application to Geology*; Malusà, M.G., Fitzgerald, P.G., Eds.; Springer International Publishing: Cham, Switzerland, **2018**, 25-48. doi:10.1007/978-3-319-89421-8_2.
23. Matteini, M.; Junges, S.L.; Dantas, E.L.; Pimentel, M.M.; Bühn, B. In situ zircon U–Pb and Lu–Hf isotope systematic on magmatic rocks: Insights on the crustal evolution of the proterozoic Goiás Magmatic Arc, Brasília belt, Central Brazil. *Gondwana Res.* **2010**, *17*, 1–12.
24. Tiepolo, M. In situ Pb geochronology of zircons with laser ablation-inductively coupled plasma-sector field mass spectrometry. *Chem. Geol.* **2003**, *199*, 159–177.
25. Gazzi, P. Sulla determinazione microscopica della composizione mineralogical delle rocce, in particolare delle arenarie e delle sabbie. *Mineral. Petrogr. Acta* **1966**, *12*, 61–68.
26. Dickinson, W.R. Interpeting detrital modes of graywackes and arkoses. *Jour. Sed. Petrol.* **1970**, *40*, 695–707.
27. Ingersoll, R.V.; Bullard, T.F.; Ford, R.D.; Grimm, J.P.; Pickle, J.D.; Sares, S.W. The effect of grain size on detrital modes: A test of the Gazzi-Dickinson point-counting method. *J. Sediment. Petrol.* **1984**, *54*, 103–116.
28. Cibin, U.; Di Giulio, A.; Martelli, L. Oligocene-Early Miocene evolution of the Northern Apennines (northwestern Italy) traced through provenance of piggy-back basin fill successions. In *Tracing Tectonic Deformation Using the Sedimentary Record*; McCann, T., Saintot, A., Eds.; The Geologoical Society: London, UK, 2003; Volume 208, pp. 269–287.
29. Dickinson, W.R. Interpreting provenance relations from detrital modes of sandstones. In *Provenance of Arenites*; Zuffa, G.G., Ed.; NATO Advanced Studies Institutes, Mathematical and Physical Sciences: Dordrecht, The Netherlands; Boston, MA, USA, 1985; pp. 165–189.
30. Gleadow, A.J.W.; Fitzgerald, P.G. Uplift history and structure of the Transantarctic Mountains: New evidence from fission track dating of basement apatites in the Dry Valleys area, southern Victoria Land. *Earth Planet. Sci. Lett*. **1987**, *82*, 1–14.
31. Gallagher, K.; Brown, R.; Johnson, C. Fission track analysis and its applications to geological problems, *Annu. Rev. Earth Planet. Sci.* **1998**, *26*, 519–572.

32. Green, P.F.; Duddy, I.R.; Gleadow, A.J.W.; Tingate, P.R.; Laslett, G.M. Fission-track annealing in apatite: Track length measurements and the form of the Arrhenius plot. *Nucl. Tracks Radiat. Meas*. **1985**, *10*, 323–328.
33. Brandon, M.T. Decomposition of mixed grain age distributions using Binomfit. *On Track* **2002**, *24*, 13–18.
34. Galbraith, R.F.; Green, P.F. Estimating the component ages in a finite mixture. *Nucl. Tracks Radiat. Meas.* **1990**, *17*, 197–206.
35. Vermeesch, P. On the visualisation of detrital age distributions. *Chem. Geol.* **2012**, *312–313*, 190–194.
36. Carrapa, B.; DeCelles, P.G.; Reiners, P.; Gerhels, G. Apatite triple dating and white mica $^{40}Ar/^{39}Ar$ thermochronology of syn-tectonic detritus in the Central Andes: A multi-phase tectono-thermal history, *Geology* **2009**, *37*, 407–410.
37. Chamberlain, K.R.; Bowring, S.A. Apatite-feldspar U–Pb thermochronometer: A reliable, mid-range (450 °C), diffusion-controlled system. *Chem. Geol*. **2000**, *172*, 173–200.
38. Schoene, B.; Bowring, S.A. Determining accurate temperature-time paths from U–Pb thermochronology: An example from the Kaapvaal craton, southern Africa. *Geochim. Cosmochim. Acta,* **2007**, *71*, 165–185.
39. Chew, D.M.; Donelick, R.A. *Apatite Fission Track And U–Pb Dating by La–Icp–Ms*; Mineralogical Association of Canada Short Course: St. John's, NL, Canada, 2012; Volume 42, pp. 219–247.
40. Chew, D.M.; Sylvester, P.J.; Tubrett, M.N. U–Pb And Th-Pb dating of Apatite By LA– ICP–MS. *Chem. Geol.* **2011**, *280*, 200–216.
41. Gehrels, G.E.; Valencia, V.; Pullen, A. Detrital zircon geochronology by Laser-Ablation Multicollector ICPMS at the Arizona LaserChron Center. In *Geochronology: Emerging Opportunities, Paleontology Society Short Course: Paleontology Society Papers*; Loszewski, T., Huff, W., Eds.; Cambridge University Press, Cambridge, UK, 2006; *11*, pp. 10.
42. Gehrels, G.E.; Valencia, V.A.; Joaquin, R. Enhanced precision, accuracy, and efficiency, and spatial resolution of U-Pb ages by laser ablation-multicollector-inductively coupled plasmamass spectrometry. *Geochem. Geophys. Geosyst.* **2008**, *9*, 1–13.
43. Gehrels, G.E. Detrital Zircon U-Pb Geochronology Applied to Tectonics. *Annu. Rev. Earth Planet. Sci*. **2014**, *42*, 127–49.
44. Thomson, S.N.; Gehrels, G.E.; Ruiz, J.; Buchwaldt, R. Routine low–damage apatite U–Pb dating using laser ablation–multicollector–ICPMS. *Geochem. Geophys. Geosyst.* **2012**, *13*, doi:10.1029/2011GC003928.
45. Ramos, V.A.; Kay, S.M. Evolution of the Andean margin: A tectonic and magmatic view from the Andes to the Neuquén Basin (35 °S–39 °S lat). In *Overview on the Tectonic Evolution of the Southern Central Andes of Mendoza and Neuquén (35 °S–39 °S Latitude*); Special Paper n. 40; Kay, S.M., Ramos, V.A., Eds.; The Geological Society of America: Boulder, CO, USA, 2006; pp. 1–17.
46. Ramos, V.A. The tectonic regime along the Andes: Present settings as a key for the Mesozoic regimes. *Geol. J.* **2010**, *45*, 2–25.
47. Tunik, M.; Folguera, A.; Naipauer, M.; Pimentel, M.; Ramos, V.A. Early uplift and orogenic deformation in the Neuquén Basin: Constraints on the Andean uplift from U–Pb and Hf isotopic data of detrital zircons. *Tectonophysics* **2010**, *489*, 258–273.
48. Balgord, E.A.; Carrapa, B. Basin evolution of upper Cretaceous-lower cenozoic strata in the Malargüe fold-and-thrust belt: Northern Neuquén Basin, Argentina. *Basin Res.* **2016**, *28*, 183–206.
49. Naipauer, M.; Ramos, V.A. Changes in Source Areas at Neuquén Basin: Mesozoic Evolution and Tectonic setting based on U-Pb ages on zircons. In *Growth of the Southern Andes*; Folguera, A., Naipauer, M., Sagripanti, L., Ghiglione, M.C., Orts, D.L., Giambiagi, L., Eds.; Springer: New York, NY, USA, **2016**; doi:10.1007/978-3-319-23060-3_3.
50. Cawood, P.A.; Hawkesworth, C.J.; Dhuime, B. Detrital zircon record and tectonic setting. *Geology* **2012**, *40*, 875–878.
51. Fennell, L.M.; Folguera, A.; Naipauer, M. Cretaceous deformation of the southern Central Andes: Synorogenic growth strata in the NeuquénGroup (35 °S 30–37 °S). *Basin Res.* **2017**, *29* (Suppl. 1), 51–72.
52. DeCelles, P.G.; Carrapa, B.; Gehrels, G.E. Detrital zircon UePb ages provide provenance and chronostratigraphic information from Eocene synorogenic deposits in northwestern Argentina. *Geology* **2007**, *35*, 323–326.
53. Martin-Gombojav, N.; Winkler, W. Recycling of Proterozoic crust in the Andean Amazon foreland of Ecuador: Implications for orogenic development of the northern Andes. *Terra Nova* **2008**, *20*, 22–31.

54. Sagripanti, L.; Bottesi, G.; Naipauer, M.; Folguera, A.; Ramos, V.A. U/Pb ages on detrital zircons in the southern central Andea Neogene foreland (36e37S): Constraints on Andean exhumation. *J. South Am. Earth Sci.* **2011**, *32*, 555–566.
55. Naipauer, M.; Tapia, F.; Mescua, J.; Farías, M.; Pimentel, M.M.; Ramos, V.A. Detrital and volcanic zircon U-Pb ages from southern Mendoza (Argentina): An insight on the source regions in the northern part of the Neuquén Basin. *J. South Am. Earth Sci.* **2015**, 1–18, doi:10.1016/j.jsames.2015.09.013.
56. Encinas, A.; Folguera, A.; Riffo, R.; Molina, P.; Fernández Paz, L.; Litvak, V.D.; Colwyn, D.A.; Valencia, V.A.; Carrasco, M. Cenozoic basin evolution of the Central Patagonian Andes: Evidence from geochronology, stratigraphy, and geochemistry. *Geosci. Front.* **2019,** *10*, 1139-1165
57. Borghi, P.; Fennell, L.; Omil, R.G.; Naipauer, M.; Acevedo, E.; Folguera, A. The Neuquén group: The reconstruction of a Late Cretaceous foreland basin in the southern Central Andes (35–37°S). *Tectonophysics* **2019**, *767*, 228177.
58. Lanteaume, M. Considérations paléogéographiques sur la patrie supposée des nappes de flysch a Helminthoides des Alpes et des Apennins. *Bull. Soc. Géol. France* **1962**, *7*, 627–643.
59. Vanossi, M.; Cortesogno, L.; Galbiati, B.; Messiga, B.; Piccardo, G.; Vannucci, R. Geologia delle Alpi liguri: Dati, problemi, ipotesi. *Mem. Soc. Geol. Ital.* **1986**, *28*, 5–75.
60. Di Giulio, A. Eo-Alpine geodynamics: An integrated approach. *Boll. Soc. Geol. It.* **1996**, *115*, 649–671.
61. Seno, S.; Dallagiovanna, G.; Vanossi, M. Pre-Piedmont and Piedmont-Ligurian nappes in the central sector of the Ligurian Alps: A possible pathway for their superposition on to the inner Briançonnais units. *Boll. Soc. Geol. Ital.* **2005**, *124*, 455–464.
62. Maino, M.; Casini, L.; Ceriani, A.; Decarlis, A.; Di Giulio, A.; Seno, S.; Setti, M.; Stuart, F. Dating shallow thrusts with zircon (U-Th)/He thermochronometry—The shear heating connection. *Geology* **2015**, *43*, 495–498.
63. Mueller, P.; Maino, M.; Seno, S. Progressive Deformation Patterns from an Accretionary Prism (Helminthoid Flysch, Ligurian Alps, Italy). *Geosciences* **2020**, *10*, 26.
64. Gasinski, A.; Slaczka, A.; Winkler, W. Tectono-sedimentary evolution of the Upper Prealpine nappe (Switzerland and France): Nappe formation by Late Cretaceous-Paleogene accretion. *Geodin. Acta* **1997**, *10*, 137–157.
65. Galbiati, B. L'Unità di Borghetto d'Arroscia-Alassio. *Mem. Soc. Geol. It.* **1984**, , 181–210.
66. Basu, A. Reading provenance from detrital quartz. In *Provenance of Arenites*; Zuffa, G.G., Ed.; Springer: Dordrecht, Netherlands, **1985**, 231–247.
67. Mueller, P.; Patacci, M.; Di Giulio, A. Hybrid event beds in the proximal to distal extensive lobe domain of the coarse-grained and sand-rich Bordighera turbidite system (NW Italy). *Mar. Pet. Geol.* **2017**, *86*, 908–931, doi:10.1016/j.marpetgeo.2017.06.047.
68. Dickinson, W.R.; Suczek, C. Plate tectonics and sandstone compositions. *Am. Assoc. Pet. Geol. Bull.* **1979**, *63*, 2164–2182.
69. Dickinson, W.R.; Beard, L.S.; Brakenridge, G.R.; Erjavec, J.L.; Ferguson, R.C.; Inman, K.F.; Knepp, R.A.; Lindberg, F.A.; Ryberg, P.T. Provenance of North American Phanerozoic sandstones in relation to tectonic setting. *Geol. Soc. Am. Bull.* **1983**, *94*, 222–235.
70. Palomares, M.; Arribas, J. Modern stream sands from compound crystalline sources: Composition and sand generation index. *Geol. Soc. Am. Spec. Pap.* **1993**, *284*, 313–322.
71. Datta, B. Provenance, tectonics and palaeoclimate of Proterozoic Chandarpur sandstones, Chattisgarh Basin: A petrographic view. *J. Earth Sci.* **2005**, *114*, 227–245.
72. Ballèvre, M.; Manzotti, P.; Dal Piaz, G.V. Pre-Alpine (Variscan) inheritance: A key for the location of the future Valaisan Basin (Western Alps). *Tectonics* **2018**, *37*, 786–817.
73. Linnemann, U.; Pereira, F.; Jeffries, T.E.; Drost, K.; Gerdes, A. The Cadomian Orogeny and the opening of the Rheic Ocean: The diachrony of geotectonic processes constrained by LA-ICP-MS U–Pb zircon dating (Ossa-Morena and Saxo-Thuringian Zones, Iberian and Bohemian Massifs). *Tectonophysics* **2008**, *461*, 21–43.
74. Casini, L.; Cuccuru, S.; Maino, M.; Oggiano, G.; Tiepolo, M. Emplacement of the Arzachena Pluton (Corsica–Sardinia Batholith) and the geodynamics of incoming Pangaea. *Tectonophysics* **2012**, 544–545, 31–49.
75. Fornelli, A.; Micheletti, F.; Piccarreta, G. Late-Proterozoic to Paleozoic history of the peri-Gondwana Calabria–Peloritani Terrane inferred from a review of zircon chronology. *Springerplus* **2016**, *5*, 1–19.

76. Manzotti, P.; Ballèvre, M.; Poijol, M. Detrital zircon geochronology in the Dora–Maira and Zone Houillère: A record of sediment travel paths in the Carboniferous. *Terra Nova* **2016**, *28*, 279–288.
77. Haas, I.; Eichinger, S.; Haller, D.; Fritz, H.; Nievoll, J.; Mandl, M.; Hippler, D.; Hauzenberger, C. Gondwana fragments in the Eastern Alps: A travel story from U/Pb zircon data. *Gondwana Res.* **2020**, *77*, 204–222.
78. Von Raumer, J.F.; Stampfli, G.M.; Bussy, F. Gondwana-derived microcontinents—The constituents of the Variscan and Alpine collisional orogens. *Tectonophysics* **2003**, *365*, 7–22.